Available online at www.sciencedirect.com
SCIENCE DIRECT
Polymer 47 (2006) 2802–2812
polymer
www.elsevier.com/locate/polymer

# Large deformation mechanical behavior of flexible nanofiber filled polymer nanocomposites

Florent Dalmas [a,b], Laurent Chazeau [a], Catherine Gauthier [a,*], Jean-Yves Cavaillé [a], Rémy Dendievel [b]

[a] GEMPPM (Groupe d'Etude de Métallurgie Physique et de Physique des Matériaux), INSA de Lyon, bât. B. Pascal, 7, av. J. Capelle, 69621 Villeurbanne cedex, France
[b] GPM2 (Génie Physique et Mécanique des Matériaux), INP Grenoble, ENSPG, BP46, 38402 St Martin d'Hères, France

Received 24 November 2005; received in revised form 23 January 2006; accepted 6 February 2006
Available online 2 March 2006

**Abstract**

In the present work, the large deformation behavior of high aspect ratio flexible nanofiber reinforced polymer composites is investigated. Simple or successive tensile tests are performed at room temperature, i.e. in the rubbery state. By studying two different types of fibers, namely cellulose nanofibrils and carbon nanotubes, with two processing routes, the role of entanglements and of interactions existing between fibers—within the nanofiber network that can be formed in the material—on the composite properties is highlighted. For cellulosic nanofillers, strong hydrogen bonds between fibers lead to a spectacular reinforcement effect combined with a decrease of the composite ultimate strain and an irreversible damage of composite properties after first deformation (rigid network). When such strong interactions between fillers are limited (soft entangled network or simple contacts between non-entangled fibers) the resulted reinforcement is less important and no decrease of the deformation at break is observed. For carbon nanotube fillers, the evolution of the filler network during tensile test is finally highlighted by in situ electrical measurements.


*Keywords:* Nanocomposites; Mechanical properties; Electrical properties

## 1. Introduction

Nanocomposite materials are made up of nanometric particles (nanofillers) dispersed in a polymer matrix. In the particular case of soft polymer matrix/stiff nanofillers systems, the mechanical reinforcement effect of these nanofillers were highlighted. Various parameters seem to be of importance in characterizing the fillers: geometrical factors such as the shape, the size, and the aspect ratio; intrinsic mechanical characteristics such as the modulus or the flexibility; surface properties such as specific surface area and surface treatment [1].

In the case of high aspect ratio fibrous nanofillers, previous experimental and theoretical studies have essentially focused on rod-like nanofibers (cf: the work of Favier et al. and Hajji et al. on cellulose whiskers as fillers in a polymer matrix [2,3]). Nevertheless, very high aspect ratio nanofibers display good flexibility properties. Dispersed in polymer matrices, they will thus create a complex entangled microstructure. The influence of the entanglement rate, the tortuosity of the fillers, their intrinsic properties and the filler–filler interactions on the composite macroscopical properties is not completely understood yet. The need for experimental study and theoretical modeling of model systems have motivated the present work.

In order to understand the effect of interactions between nanofibers, two different types of flexible nanofibers were used: cellulose nanofibrils and carbon nanotubes. Moreover, by using two different processing conditions, entanglements and contacts between nanofibers could be modified.

The cellulose is a semi-crystalline biopolymer (with a relative density of 1.58 g cm$^{-3}$), naturally synthesized as nanofibrils, which constitutes the rigid skeleton of numerous species such as plants, some alga or mushrooms and amoebae [4–6]. Eichhorn and Young [7] have measured by in situ Raman spectroscopy a value of 25 GPa for the longitudinal Young's modulus of cellulose fibrils. Despite their interesting mechanical properties and the progress made for their extraction and their individualization from natural materials

* Corresponding author. Tel.: +33 4 72 43 83 57; fax: +33 4 72 43 85 28.
*E-mail address:* catherine.gauthier@insa-lyon.fr (C. Gauthier).

0032-3861/$ - see front matter © 2006 Elsevier Ltd. All rights reserved.
doi:10.1016/j.polymer.2006.02.014

[8], cellulose nanofibrils were, up to now, poorly studied as fillers in polymer matrices [9].

Concerning carbon nanotubes, papers related to their use in nanocomposite materials are more and more numerous since their discovery by Ijima in 1991 [10]. Even if experimental studies [11–13] and theoretical modeling [14–16] have demonstrated high Young's modulus (of the order of magnitude of 1 TPa) and stiffness of carbon nanotubes, their real efficiency as a means to increase the mechanical reinforcement in polymer matrices is still an open question as suggested by the diversity of the results found in the literature [17–21]. In addition to their outstanding mechanical properties, carbon nanotubes are good electrical conductive objects [22]. Dispersed in an insulating matrix, they allow the material to be conductive above a certain nanotube content, called the electrical percolation threshold; but, here again, results in the literature are very scattered [23–26].

Nanocomposites with an amorphous thermoplastic matrix reinforced by cellulose nanofibrils and multi-walled carbon nanotubes (MWNTs) were recently synthesized [27]. Two processing routes were used to elaborate nanocomposite materials: an aqueous mixture of polymer latex and nanofiber suspension was either evaporated or freeze-dried and pressed. A dynamic mechanical analysis of these composites was previously performed [27]. In the case of cellulose filled nanocomposites, a large mechanical reinforcement effect was measured. Moreover, a significant increase in materials flowing temperature was observed. Indeed, composites filled with high cellulose contents displayed a large rubbery plateau (at a high modulus level) even for high temperatures where the matrix is completely viscous. These effects were explained by the formation of a rigid nanofibril network linked by hydrogen bonds [2], which prevents the polymer flowing and leads to a strong mechanical reinforcement. A mechanical percolation model was successfully used to take into account the presence of this rigid fiber network within the soft polymer matrix. Conversely, when such bonds between cellulose fibrils were prevented by the process, a lower mechanical reinforcement is observed and can be modeled by a classical mean field approach. On the other hand, both types of composites filled with carbon nanotubes (where no strong interactions are possible) highlighted the fact that entanglements are responsible for a strong increase in thermo-mechanical stability but do not influence the mechanical reinforcement. Thus, two main effects were differentiated: the effect of fiber entanglements on thermo-mechanical properties and the effect of the contact strength on the mechanical reinforcement level.

In the particular case of carbon nanotubes (which are good conductive objects [28]) filled materials, electrical properties were also investigated. The processing conditions were found to strongly influence the electrical efficiency of tube/tube contacts. Indeed, when the composites are prepared by the freeze-drying method, a lower conductivity level is measured, compared to that of the composites made by evaporation.

To fully understand the influence of fiber entanglements and fiber/fiber interactions on the filler network properties, more informations are needed. In order to study the damage of this fiber network in polymeric nanocomposites, large deformation measurements at temperature above the polymer glass transition temperature are now of interest.

Thus, the purpose of the present work is the mechanical study of such nanocomposites in the non-linear domain. Classical tensile tests are performed above the glass transition temperature ($T_g$) of these composites. The role of the damage of a possible fiber network is discussed on successive tensile tests. The existence of this network and its interaction with the matrix are investigated by swelling experiments. For MWNTs filled materials, the Ac electrical properties are measured in situ during tensile test for different frequencies of the applied electrical field.

## 2. Experimental

### 2.1. Materials

#### 2.1.1. The nanofillers

Cellulose nanofibrils were obtained from sugar beet pulp at the CERMAV (Centre de Recherche sur les Macromolécules Végétales, CNRS, B.P. 53, 38041 Grenoble Cedex, France). The chemical treatment used is described by Dinand et al. [8]. This treatment allows to obtain a final aqueous suspension of cellulose nanofibrils, which does not sediment or flocculate. A TEM observation of these cellulosic fibrils is presented in Fig. 1(a). Because of cellulose degradation under the electronic beam, their TEM high magnification observations are really difficult to obtain. Nevertheless, one can observe in Fig. 1(a) that cellulose nanofibrils are arranged in bundles of 10–50 nm width. Such a bundle structure of cellulose nanofibrils makes impossible the estimation of the nanofibrils mean length by TEM imaging at low magnification.

MWNTs were synthesized at EPFL from the catalytic decomposition of acetylene at 720 °C on supported cobalt/iron catalyst as already described [29]. For purification, raw MWNTs sample was sonicated in 30% $HNO_3$ for 3 h then filtered and washed with distilled water and finally dried at 120 °C. As shown in Fig. 1(b), the purified multi-walled carbon nanotubes used in this study are very long (the nanotubes mean length was estimated on low magnification TEM images to be around 10 μm), flexible and entangled. Couteau and co-workers [29] previously showed by EDX (energy dispersive X-ray) analysis that with this purification process the Fe ($K_\alpha$ 6.4 eV and $K_\beta$ 7.06 eV) and Co ($K_\alpha$ 6.93 eV and $K_\beta$ 7.65 eV) peaks are drastically reduced in the purified sample. This means that the metallic catalysts are mainly removed by the purification step. Image analysis made on several TEM pictures gives a diameter distribution between 8 and 100 nm with a mean value around 32 nm. Thus, the mean aspect ratio of these carbon nanotubes can be estimated to be $240 \pm 70$. The relative density of MWNTs can be estimated to 2 g cm$^{-3}$ by taking into account the volume of graphite (relative density 2.2 g cm$^{-3}$) in a nanotube.

The purified nanotubes were dispersed in a distilled water solution of 1.2 g L$^{-1}$ sodium dodecylbenzene sulfonate

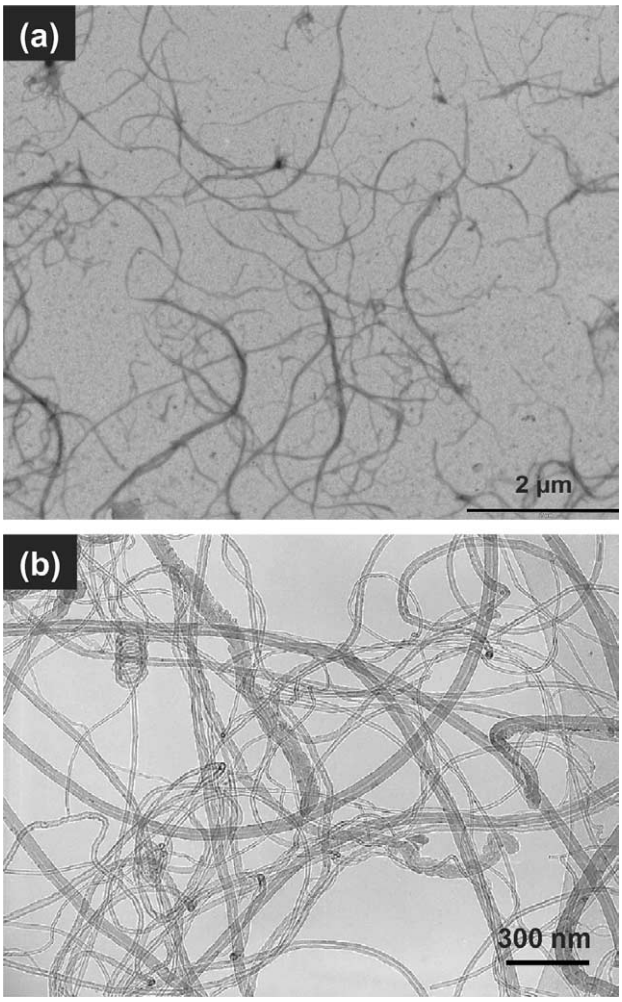


Fig. 1. TEM observation of (a) cellulose nanofibrils extracted from sugar beet, and (b) purified multi-walled carbon nanotubes.

(SDBS: $C_{18}H_{29}SO_3Na$) surfactant using a sonication step for 5 min with 20 mL suspension volumes, using a Branson Sonifier with a 13 mm probe tip at 20 kHz and a power source of 25 W. Several weight ratios of nanotubes to surfactant were investigated for solution stability and an optimum ratio of five (5:1) was chosen to obtain an aqueous suspension stable for at least 3 weeks. The resulting nanotubes concentration in the suspension is 5 g $L^{-1}$.

### 2.1.2. Composite processing

The latex was prepared by emulsion copolymerization of styrene (35 wt%) and butyl acrylate (65 wt%) using a semi-continuous feed process (LCPP, Laboratoire de Chimie et Procédés de Polymérisation, UMR CNRS 140—CPE Lyon, BP 2077, 69616 Villeurbanne Cedex, France). The polymerization occurs in a miscellar aqueous solution of a surfactant mixture: an anionic ($C_{12}H_{25}O(CH_2CH_2O)_4SO_3Na$) and a non-ionic ($C_{12}H_{25}O(CH_2CH_2O)_{19}H$). A surfactant-stabilized aqueous suspension of poly(styrene-co-butyl acrylate), P(S-BuA)—with a relative density of 1.07 g $cm^{-3}$—is obtained containing 43 wt% of spherical polymer particles with an average diameter of $145 \pm 10$ nm (determined by light scattering). The glass transition temperature of P(S-BuA) was determined by differential scanning calorimetry (heating rate of 10 K $min^{-1}$) and found to be 266 K.

The latex was first stirred with the stable aqueous suspension of nanofillers. Two processing conditions were then used to prepare the composites. The mixture was either cast in an aluminum mold with a teflon coating and put in a drying oven at 308 K under vacuum for 5 days. The chosen temperature (about 40 K above the polymer glass transition temperature) allows the water evaporation and the film formation (i.e. polymer particles coalescence). So-called evaporated films (or materials *E*) were obtained. For the second route used to elaborate composites, the mixture was first freeze–dried to allow water sublimation, a compact soft powder was obtained. This powder was then pressed at 373 K for 5 min under 1 MPa after 45 min of thermal stabilization without pressure. This second type of nanocomposite materials is referred as FP materials. In both cases, the chosen parameters allow to obtain homogeneous composite samples and transparent pure P(S-BuA).

Samples reinforced with nanofillers contents of up to 6 vol% for cellulosic nanofibrils or up to 3 vol% for MWNTs fillers, were processed. Parallelepipedic samples (around $5 \times 15 \times 0.7$ $mm^3$) were cut for mechanical testing.

The good level of dispersion of nanofillers within the P(S-BuA) matrix can be seen on Fig. 2 which shows an example of TEM observations on thin composite microsections. Indeed, no aggregate can be observed and both nanotubes and nanofibrils seem to be homogeneously distributed within the matrix. It is noteworthy that on a composite microsection, nano-fibers seem to be shorter and less entangled than what they are really in the corresponding macroscopic sample, because of the small observed thickness.

### 2.2. Methods

The non-linear mechanical behavior was analyzed via tensile tests. Measurements were performed on a MTS device (MTS 1/ME). A thermo-regulated chamber allowed to work in a temperature range from −70 to 300 °C. Constant cross head speeds of 18 or 2.5 mm $min^{-1}$ were maintained, corresponding to initial strain rates of $2 \times 10^{-2}$ or $2.7 \times 10^{-3}$ $s^{-1}$, respectively. True stress $\sigma$ and true strain $\varepsilon$ were given by the relationships:

$$\varepsilon = \ln\left(\frac{L}{L_0}\right) \text{ and } \sigma = \frac{FL}{S_0 L_0} \quad (1)$$

where $L_0$ was the initial sample length, $L$ was the length during the test and $S_0$ the initial sample section. The stress is calculated with the assumption of volume conservation. For high strain level, this assumption is questionable. Nevertheless, the calculation with a constant sample cross-section (i.e. with the assumption of the maximum increase of the sample volume during stretching) gives the same evolution of the stress–strain

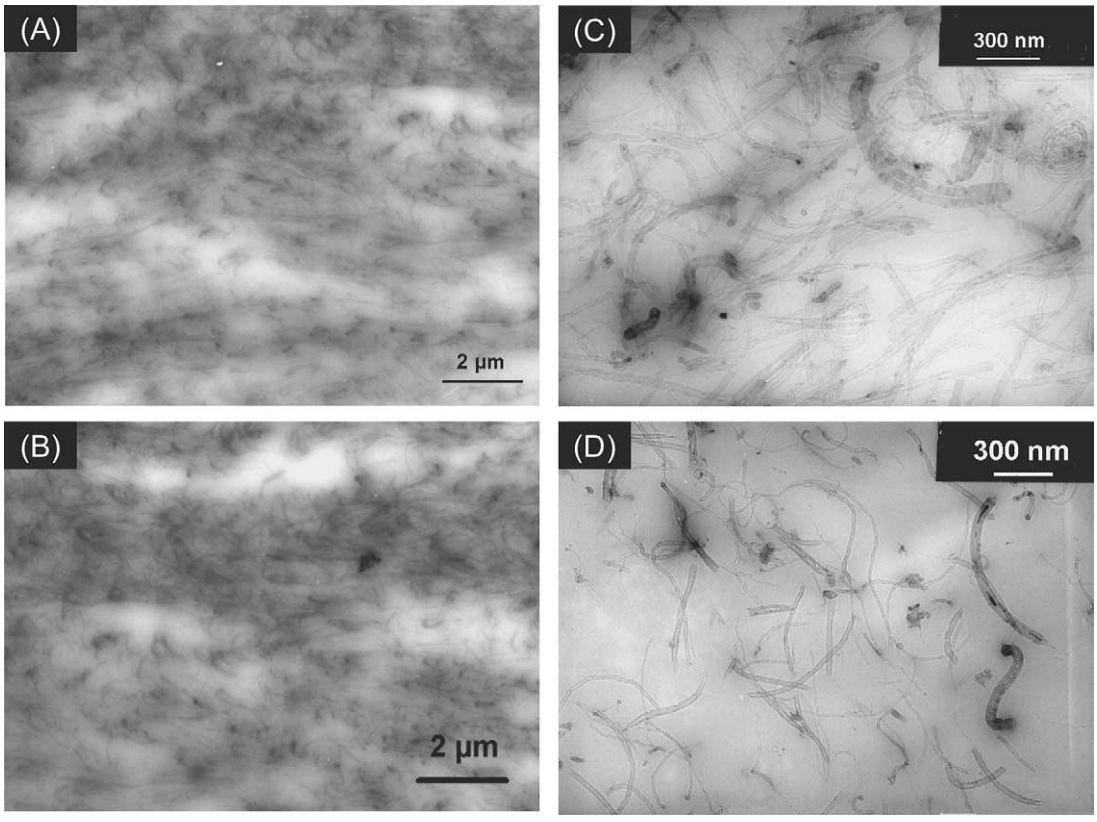


Fig. 2. Low magnification TEM micrographs of microsections from a P(S-BuA) film filled with 4 vol% of cellulose nanofibrils *E* (A) or FP (B), and with 3 vol% of MWNTs *E* (C) or FP (D).

curves, only shifted toward lower stress levels. Thus, qualitative discussions concerning the effect of filler content on mechanical behavior and on mechanical reinforcement are not impacted by this assumption. For each testing conditions, five samples were tested. In the following, the given results represent average values of modulus or the more representative tensile curves.

Swelling experiments were run in order to evaluate the interactions between the fillers and the polymer matrix. Toluene was chosen because it is a good solvent of both polystyrene and poly(butyl acrylate). A parallelepipedic shaped sample of weight $m_i$ (around 0.2 g) was immersed in toluene for 2 days. Once swollen, the sample was extracted (when possible), dried at 30 °C for 1 day and weighted (weight $m_d$). The weight fraction $G$ of residual gel in the composite after swelling is then given by

$$G = \frac{m_d}{m_i}\left(\frac{1}{Q}+1\right) - \frac{1}{Q} \tag{2}$$

where $Q$ is the ratio of the polymer weight to the filler weight for the composite sample.

In situ electrical conductivity measurements were carried out during a tensile test, as already done for other conductive nanocomposites [30]. Samples were coated at their ends with a silver paint to ensure a good electrical contact. Electrodes and samples were carefully isolated from the tensile machine. Longitudinal Ac complex electrical conductivity measurements were performed at ambient temperature for several frequencies ranging from 10 to 1 MHz using a Solartron 1226 bridge with a low applied field of about 1 V cm$^{-1}$. The complex admittance $Y^*$ was recorded versus time. From this admittance, the conductivity $\sigma_e^*$ can be deduced following the equation

$$\sigma_e^* = Y^* \frac{L}{WT} = Y^* \frac{L^2}{V_0} \tag{3}$$

with $W$, $L$ and $T$ the width, the length and the thickness of the sample during the test, and $V_0 = L_0 \times T_0 \times W_0$ the sample initial volume. The conductivity in place of the admittance was chosen to be plotted in results presentation because it is an intrinsic parameter that should remain constant without any changes in the arrangement of the conductive component, conversely to the admittance, which depends on the geometry variation of the samples. Note however, that the Eq. (3) uses the assumption of a constant volume of the sample during stretching. This will be discussed below.

## 3. Results and discussion

### 3.1. Tensile tests

Monotonic tensile tests were performed on pure P(S-BuA) and related composites with a cellulose nanofibril content up to 6 vol%. The initial strain rate was $2\times10^{-2}$ s$^{-1}$ (which corresponds to a crosshead speed of 18 mm min$^{-1}$). The tests were performed at room temperature, that is around 30 K

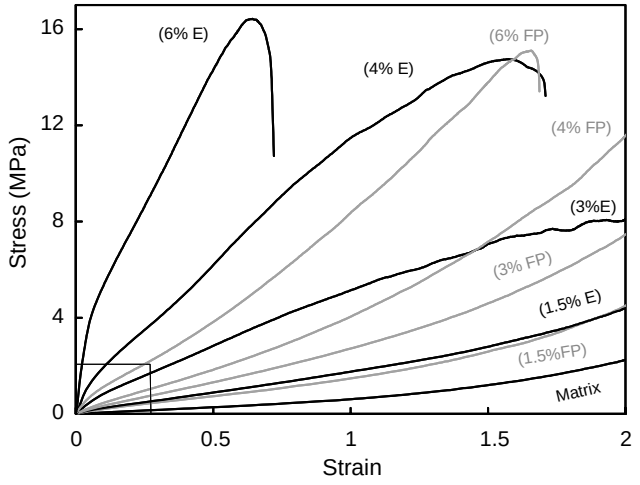


Fig. 3. Tensile tests performed at room temperature with an initial strain rate of $2\times10^{-2}\,s^{-1}$ on pure P(S-BuA) matrix and related cellulose filled composites either *E* (black lines) or FP (gray lines). The cellulose contents are given in volume percentage.

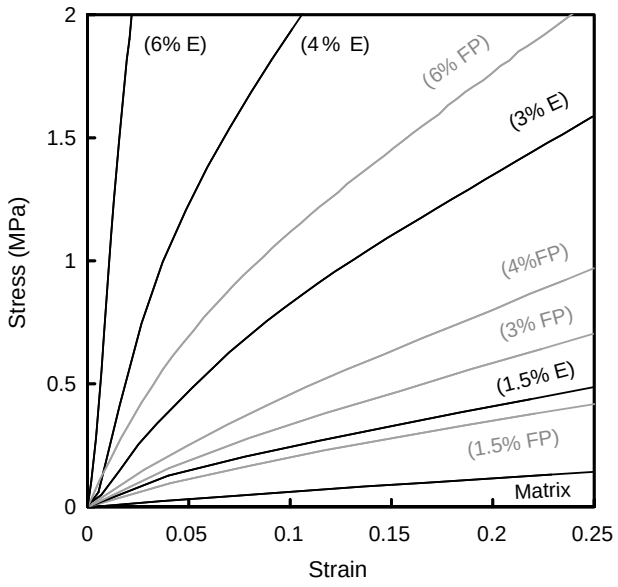


Fig. 4. Initial portion of the stress–strain curve of Fig. 3 obtained on pure P(S-BuA) matrix and related cellulose filled composites either *E* (black lines) or FP (gray lines). The cellulose contents are given in volume percentage.

above $T_g$ and the resulting stress–strain curves are presented in Fig. 3. The very last part of the curve (for true strain > 2, i.e. stretching > 650%) was found to be not reproducible for the five different samples tested for each material. Indeed, some samples present an increasing stress up to the maximum crosshead displacement available with the apparatus, whereas other samples from the same material can reach a maximum stress and then display a decreasing stress. For such high strain levels, the sample becomes extremely thin and it becomes impossible to check the homogeneity of the deformation in the sample. That is the reason why, the results are not discussed in this range of strain and the curves in Fig. 3 are stopped at $\varepsilon = 2$.

The unfilled P(S-BuA) exhibits the typical behavior of amorphous thermoplastic above $T_g$, i.e. a rubber-like non-linear elastic behavior, which is found independent on processing conditions. For such an amorphous polymer without cross-linking, no fracture is observed and the stress–strain curve continues until the flow of the sample. In the case of composites filled by 1.5 vol% of nanofibrils, the same kind of rubber-like behavior as in the matrix is observed but with higher stress level. Here again, this is independently on processing conditions. On the other hand, *E* composites filled with 3, 4 and 6 vol% of nanofibrils display a different behavior. Indeed, the 4 and 6 vol% filled materials exhibit a pseudo-plastic behavior with a slope change in their stress–strain curve. These composites present a fracture point with an ultimate strain quickly decreasing with the nanofibril content. The 3 vol% filled materials have an intermediate behavior between that of the rubber-like matrix and that of the pseudo-plastic composites with higher cellulose contents.

The Young's modulus values were analysed from the initial slope of the tensile curves, as detailed in Fig. 4. For the *E* systems, the Young's modulus was found to non-linearly increase with the nanofibril content; i.e. by about 150 times when only 6 vol% of nanofibrils is used, and by only four times when 1.5 vol% of nanofibrils is added. This discrepancy can be explained by the presence of strong interactions, through hydrogen bonds, between cellulose nanofibrils.

Previously [27], a simple isotropic calculation using the Halpin–Tsai equation was made. Such a model is a mean field approach for isotropic stiff straight fiber composites, which assumes that the fibers have no interaction with their neighbors [31]. Data taken from the literature for cellulose fibrils [32] were used for the fiber parameters, i.e. a longitudinal modulus $E_{f11}$ equal to 30 GPa and transversal moduli $E_{f22}$ and $E_{f33}$ equal to 15 GPa; and the fiber aspect ratio was set to 300 (even if high resolution electron microscopy on cellulosic objects is impossible, this aspect ratio value seems to be reasonable regarding Fig. 1(a)). Then, the Young's moduli calculated by this mean field approach was found to be strongly lower than the experimental ones obtained on *E* cellulose filled composites. Thus, this suggests that in *E* composites strong interactions exist between nanofibers, and are responsible for the measured high mechanical reinforcement. As already observed by Favier et al. [2] and Hajji et al. [3] for nanocomposites with the same matrix reinforced by cellulose whiskers, cellulose nanofibers are organized in a rigid network linked by hydrogen bonds when filler content is above the percolation threshold. This percolation threshold was theoretically estimated to be 1 vol% for straight cellulose whiskers with an aspect ratio of 100 [33]. Cellulose nanofibrils are longer than cellulose whiskers and present a higher aspect ratio and consequently, a lower percolation threshold. Therefore, all the composites tested in the present paper have cellulose content above the percolation threshold. The high Young's modulus and the lower ultimate strain of such composites is governed mainly by nanofibril strong interactions, i.e. by the rigid cellulose network formed within the soft matrix. The slope change observed in the stress–strain curves for composites containing 3, 4 or 6 vol% of nanofibrils is then

related to the partial breakage of this network. Moreover, the addition of nanofillers seems to be responsible for a damage of the polymer matrix. Indeed, materials filled with high cellulose content present a break point; the strain level at this point decreases while the cellulose content increases.

Conversely, for high filler contents, FP composites exhibit a different mechanical behavior compared to the *E* ones. Previous works [2,27] have highlighted the fact that the freeze–drying process prevents, or at least strongly limits, the creation of strong hydrogen bonds between cellulose nanofibers. Indeed, at the beginning of the process, nanofibers are dispersed in a diluted suspension where they can be considered isolated from each other. Then, during the slow evaporation, because of Brownian motions in the suspension (whose viscosity remains low, up to the end of the process when the particle concentration becomes very high), the rearrangement of the nanofibers is possible. The resulting structure (after the coalescence of polymer particles) is completely relaxed and direct contacts between the long and flexible nanofibers are then created. Conversely, during the FP process, the particle arrangement in the suspension is first frozen, and then, during the hot-pressing, because of the melted polymer viscosity, the nanofiber rearrangements are strongly limited. Thus, in this last case, contacts are made through a certain amount of polymer matrix. Consequently, except for 6 vol% of cellulose content, the FP materials present in Fig. 3 a mechanical behavior similar to that of the unfilled matrix but with higher stress levels. No decrease of the material ultimate strain is observed and the model previously described allowed to model the Young's modulus of these FP composites. This confirms that no rigid cellulose network is created within the matrix, because of the lack of strong interactions between cellulose nanofibrils. Note that the 6 vol% cellulose filled FP composite constitutes a particular case because of its mechanical behavior intermediate between the most rigid 6 vol% *E* materials and the pure matrix. Although the FP process limits the creation of hydrogen bonds, some bonds may evenly be created during the process. For high cellulose contents these some hydrogen bonds are numerous enough to influence the overall composite mechanical behavior.

Tensile test results of MWNTs filled materials are plotted in Fig. 5 (here again, because of reproducibility problems, the curves are stopped at $\varepsilon = 1.5$). These results are comparable to that previously described for FP cellulose filled composites. Indeed, due to their surface chemistry, carbon nanotubes cannot create strong links among each other. Thus, the same rubber-like behavior as the matrix is obtained for composites, with a mechanical reinforcement lower than for *E* cellulose filled composites and which can be modeled by a Halpin–Tsai type calculation. Moreover, no difference can be observed in Fig. 5 between *E* and FP material for both nanotube contents.

Previous dynamic mechanical analysis (DMA) performed on such MWNT reinforced materials [27] have shown a lower flowing temperature for FP materials (380 vs. 430 K for *E* materials). An assumption of a lower nanotube entanglement rate resulting from the FP process was then made to explain this difference. The presence of an entangled nanotube network (a soft network, without strong links) in *E* materials is responsible for the composite elastic modulus in high temperature range where the polymer matrix is viscous. During the FP process, nanotubes do not have time to reorganize and to create entanglements; they remain isolated from each other. However, the mechanical reinforcement at room temperature was found to be independent on these entanglements and to be only due to stress transfer. The tensile behavior at room temperature also appears independent on the process. At large deformation the mechanical properties of the soft entangled nanotube network are certainly negligible compared to the stress transfer resulting from interactions between nanotube surface and the polymer chains.

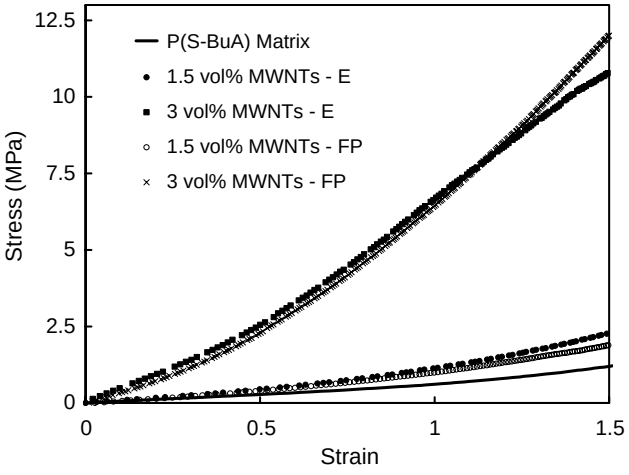


Fig. 5. Tensile tests at room temperature for carbon nanotubes filled P(S-BuA) composites either *E* or FP, with an initial strain rate of $2\times10^{-2}\ s^{-1}$.

Fig. 6 displays tensile tests performed on 3 vol% MWNTs filled composites *E* and FP at 373 K. For this high temperature, *E* and FP composites do not show the same behavior. In this range of temperature the P(S-BuA) matrix behaves as a viscous

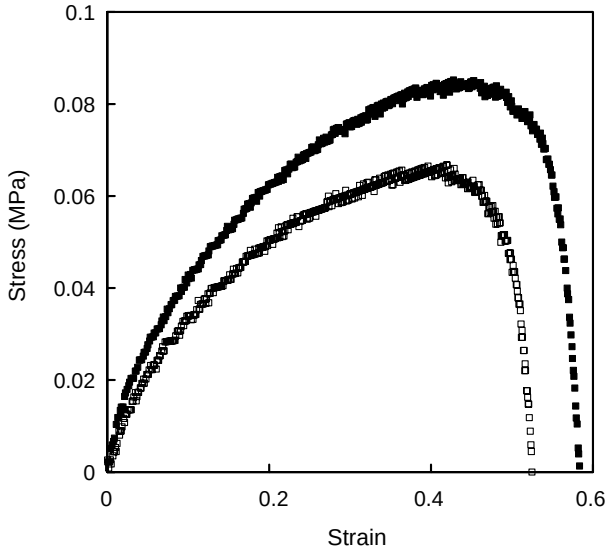


Fig. 6. Tensile tests performed with an initial strain rate of $2\times10^{-2}\ s^{-1}$ at $T=$ 373 K for P(S-BuA) composites filled with 3 vol% of MWNTs either *E* (■) or FP (□).

fluid. Nevertheless, composites still display an elastic response for this temperature. As discussed previously, this observation, which is in agreement with DMA data, can be explained by the presence of an entangled nanotube network in *E* materials. In FP ones, where the assumption of few nanotube entanglements was made, tube/tube interactions may exist at the simple contact between tubes (through the polymer or maybe the surfactant) and can explain the existence of the composite mechanical response at such a high temperature. Nevertheless, at this temperature, the higher mechanical properties of tube/tube entangled contacts compared to simple contacts are highlighted by the higher Young's modulus and the higher yield strain and stress obtained for the *E* material.

For temperatures higher than 380 K, DMA results showed [27] that simple contacts between nanotubes (in FP systems) lead to the flow of the material and entangled contacts (*E* systems) are responsible for the material elastic properties.

### 3.2. Swelling experiments

To check these assumptions, swelling experiments were performed on these nanocomposites. Fig. 7 presents the gel fraction from swelling measurements for all composite systems. The unfilled matrix is completely dissolved by the toluene and no residual gel is recovered at the end of the swelling experiment. Thus a gel fraction $G=0$ means complete dissolution of the material. For cellulose filled *E* composites, this dissolution becomes partial ($G>0$) even for small amount of nanofibrills added. The gel fraction increases with the filler content. One can observe differences with FP cellulose filled materials: firstly, the gel fraction is lower than for *E* materials; and with 4 and 6 vol% of cellulose, the FP composites are disintegrated after swelling whereas for the same cellulose contents the *E* composites keep their cohesion. Concerning MWNTs filled composites, all FP materials are completely dissolved in toluene; while only the 3 vol% reinforced *E* composite presents a residual gel fraction after swelling but with disintegration of the film.

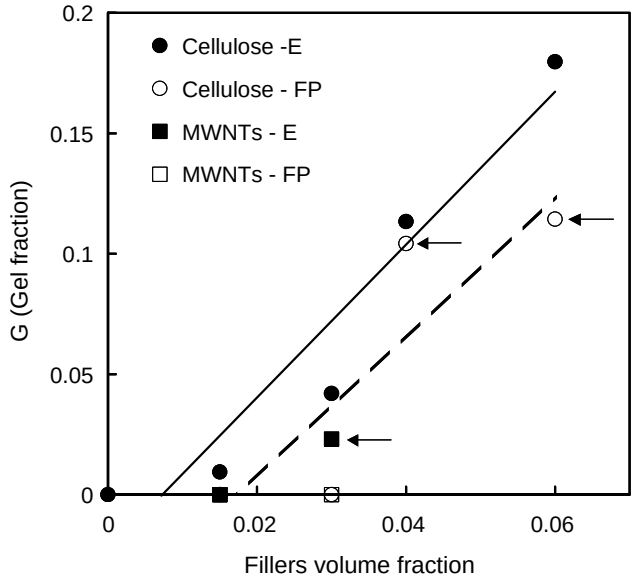


Fig. 7. Gel fraction in composite materials as a function of filler content from swelling measurements. Points marked with an arrow are for disintegrated samples. The average linear behavior for *E* (solid line) and FP (dotted line) cellulose filled materials are represented.

The existence of a non-soluble gel fraction in toluene for some composites could be related to the presence of a rigid nanofiller network. Thus, when this network does not exist (filler content below the percolation threshold in *E* cellulose filled composites) or when this network is no strong enough (FP low content cellulose filled, FP MWNTs filled or *E* 1.5 vol% MWNTs filled systems), no gel fraction is measured, that is the reason why the average lines in Fig. 7 does not go through zero. The fact that this non-soluble gel fraction can be disintegrated or not after swelling is the result of the cohesion of this network. Thus, for *E* cellulose filled composites, the presence of the rigid network is confirmed. Indeed, the solvent does not have any effect on the hydrogen bonds of the cellulose network and the sample is not desintegrated. When less strong interactions are created between the nanofibrils (FP cellulose filled composites), the polymer chains can more easily be disentangled and dissolved by the solvent. However, as previously assumed, some hydrogen bonds can be created during the FP process and are responsible for the disintegrated recovered gel fraction in such systems. In the case of MWNTs filled materials, the measured gel fraction in the 3 vol% filled materials reveals the presence of an entangled nanotube network. Nevertheless, the poor mechanical properties of this network (in comparison with the rigid cellulose network) lead to the disintegration of the film after swelling. In the FP nanotube filled materials, where such an entangled network does not exist, interactions between nanotubes surface and polymer chains are not strong enough to prevent the polymer dissolution in the solvent.

To conclude, the swelling measurement are in very good agreement with the scheme previously proposed to explain tensile test results.

### 3.3. Cyclic tensile tests

Successive tensile tests were performed at room temperature at the same strain rate ($2\times10^{-2}\,s^{-1}$) as for the simple tensile tests previously presented. The experiments consisted of loading the material up to a true deformation $\varepsilon_1=0.25$ (test with a previous strain of 0). Then the material is slowly unloaded to a stress equal to 0, and then relaxed at room temperature during 45 min. This procedure was repeated three times with increasing $\varepsilon_i$ by steps of 0.25 (test with previous deformation $\varepsilon_{i-1}$). For each tensile test the sample is considered as a new sample with new dimensions, even if a permanent strain remains. The values of the Young's modulus, *E*, measured from these successive tensile tests for *E* and FP composites filled with 1.5, 3 and 4 vol% of cellulose are shown in Table 1. No strong damage in the mechanical properties of the 1.5 vol% cellulose filled *E* composite is observed, the modulus appears constant wathever the previous strain. On the

Table 1
Evolution of the tensile Young's modulus (in MPa) with the previous strain for different cellulose nanofibril contents in nanocomposites either *E* or FP

| Process | Cellulose content (vol%) | Previous strain | | | |
|---|---|---|---|---|---|
| | | 0 | 0.25 | 0.5 | 0.75 |
| *E* | 1.5 | 2.6 | 3.1 | 2.5 | 2.1 |
| | 3 | 17.3 | 10.8 | 6.9 | 6.4 |
| | 4 | 39.8 | 23.5 | 18.6 | 11.1 |
| FP | 1.5 | 2.4 | 1.9 | 1.8 | 1.2 |
| | 3 | 2.9 | 5.0 | 3.2 | 3.2 |
| | 4 | 11.6 | 6.6 | 4.8 | 4.5 |

other hand, when 3 and 4 vol% of cellulose nanofibrils are added in *E* materials, the modulus strongly decreases with the previous strain. As supposed before, for these cellulose contents, a rigid nanofiller network is present within the composites. Such a network is broken at low strain level, for a true strain around 0.05, as shown by the slope change observed in Figs. 3 and 4 for composites containing 3, 4 or 6 vol% of nanofibrils (this value is consistent with the results of Dufresne et al. [34] who showed that the fracture of paper sheet made with the same sugar beet nanofibrils occurs at a strain of 0.1). Thus after the first test, the cellulose network is damage in *E* composites, i.e a large number of hydrogen bonds between fibrils are broken. This irreversible damage increases with the pre-strain value, and leads to a lower Young's modulus. It is interesting to notice that, for *E* composites, the last tensile test (pre-strain of 0.75) gives modulus values in the same range of order as those of FP samples. This means that after the two first cycles, all strong bonds between nanofibrils are broken, and then, the *E* composites behave as the FP composites, i.e. materials filled with cellulose nanofibrils without strong links between fibrils. Indeed, for FP systems, no rigid nanofibril network was expected, as previously highlighted. Thus, the Young's moduli are lower as previously observed in Fig. 3. For low cellulose content, the modulus can be considered as constant (regards to the variance of the different samples tested) with the pre-deformation, the mechanical reinforcement being only due to stress transfer, no damage of the filler/filler interactions is observed. Only the modulus of the 4 vol% filled material is significantly decreased by the pre-deformation. As observed before in swelling experiments, for high cellulose contents, some hydrogen bonds between neighbor fibers can certainly be created even during the FP process. These bonds are mainly broken after the first pre-deformation as shown by the weak difference in Young's modulus for the three last tensile tests on the 4 vol% cellulose filled FP composites.

For MWNTs filled materials, the same modulus level is observed between *E* and FP composites in Table 2. As no strong interactions are created between carbon nanotubes, the modulus of the composites is not significantly influenced by the pre-strain value (the Young's modulus values are scattered but can be considered as constant regards to experimental uncertainties). Moreover, the difference in entanglement rate previously assumed between *E* and FP materials does not have an influence on these results. Indeed, as for monotonic tensile tests, the nanotube entangled network might not be strong enough compared to the matrix modulus at room temperature to have an effect on the composite behavior. One can suppose that this network can be disentangled for a low applied stress.

Table 2
Evolution of the tensile Young's modulus (in MPa) with the previous strain for different carbon nanotube contents in nanocomposites either *E* or FP

| Process | MWNT content (vol%) | Previous strain | | | |
|---|---|---|---|---|---|
| | | 0 | 0.25 | 0.5 | 0.75 |
| *E* | 1.5 | 2.1 | 0.5 | 1.0 | 1.2 |
| | 3 | 7.8 | 8.6 | 8.8 | 6.3 |
| FP | 1.5 | 1.0 | 0.7 | 0.9 | 0.8 |
| | 3 | 4.7 | 8.1 | 6.3 | 5.8 |

### 3.4. In situ electrical measurements

As carbon nanotubes are good electrical conductive objects, the Ac electrical conductivity for different frequencies of the 3 vol% MWNTs filled composites was followed during the tensile test in order to investigate the microstructural evolution in such materials. In order to measure enough points of conductivity during the deformation, these experiments were performed with a deformation rate (initial strain rate of $2.7\times 10^{-3}\,s^{-1}$) slower than that of tensile tests previously presented. The corresponding stress–strain curves and the evolution of the real and imaginary parts of the conductivity with the strain for these coupled measurements are presented on Fig. 8 for *E* and FP composites. As already observed in Fig. 5, almost no difference in mechanical behavior exists between *E* and FP composites. For this slow strain rate, the materials present a yield point for a true strain around 1. Note that the evolution of the electrical conductivity is calculated by assuming that the sample volume remains constant during the deformation. As discussed previously, this assumption does not modify the results discussion, indeed by calculating the conductivity evolution with a constant sample cross-section (i.e. with the assumption of the maximum increase of the sample volume during stretching), the same conductivity range and the same evolution with the strain were obtained, only shifted toward lower strain levels.

First, it can be observed in Fig. 8 that the *E* composite remains conductive until a high strain level, $\varepsilon = 1.2$ (which corresponds to the yield point of the material as shown in Fig. 8). Indeed, in this region, the real part of the conductivity is very high, of an order of magnitude of $20\,S\,m^{-1}$, and independent of the frequency. This indicates a resistive behavior. As previously discussed for frequency dependence measurements on the unstrained samples [27], this high level of electrical conductivity combined with a resistive behavior is related to the presence of a carbon nanotube percolating network within the matrix; the experimental percolation threshold was found to be 0.2 vol%. One can observe a small increase in the real conductivity at the beginning of the deformation that can be due to a rearrangement of the nanotubes, which in turn leads to an increase of contact

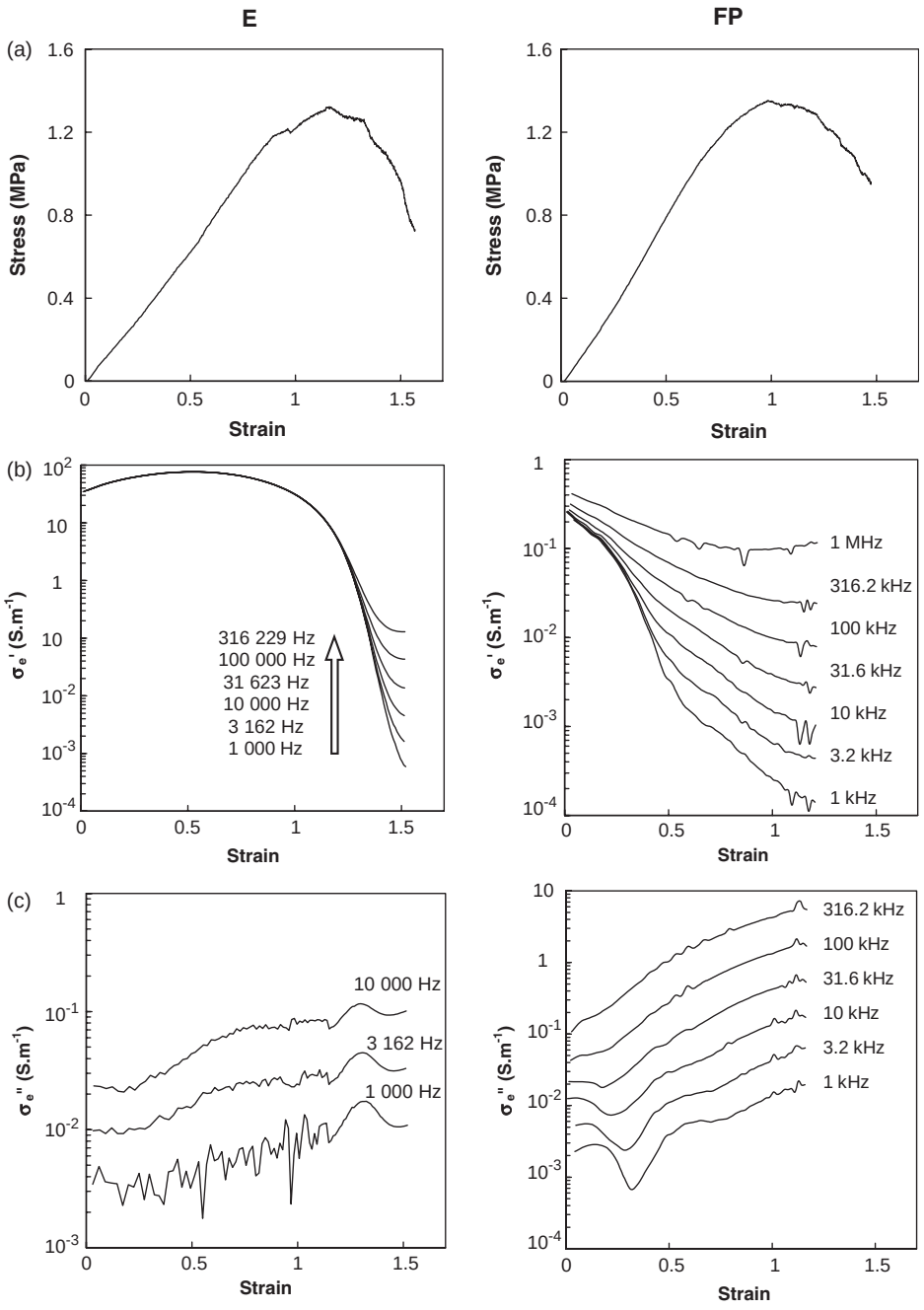


Fig. 8. In situ electrical measurements performed with an initial strain rate of $2.7\times10^{-3}$ s$^{-1}$ at room temperature for P(S-BuA) composites filled with 3 vol% of MWNTs either *E* or FP. Evolution of the Stress (a), the real (b) an imaginary (c) part of the electrical conductivity at different frequencies with the true strain.

nodes between neighboring nanotubes. After reaching a maximum, the real conductivity slowly decreases with increasing strain while the imaginary part increases, up to the yield point of the material. At this deformation level, $\sigma'_e$ begins to strongly decrease and becomes dependent on the frequency whereas $\sigma''_e$ passes through a peak which is indicative of a damage in the percolating network. Indeed, this peak of $\sigma''_e$ corresponds to a maximal capacitive effect in the composite, the nanotubes are then not in resistive contact any more, but form capacitances between them. At higher deformation levels, the material is damaged, i.e. the connective network of nanotubes responsible for electrical percolation is broken, as shown by the dielectric behavior of the material in the same conductivity range of order as the pure P(S-BuA) matrix.

Although their tensile mechanical behavior appeared similar at room temperature, *E* an FP composites display strong differences in their electrical properties. First, in Fig. 8(b), one can observe that the unstrained FP composite present a lower conductivity than the *E* one with the same MWNTs content (35 S m$^{-1}$ for the *E* composite versus 0.3 S m$^{-1}$ for the FP). Moreover, the unstrained FP composite has a capacitive behavior, as shown by the small increase of $\sigma'_e$ with the frequency, whereas the *E* composite is completely resistive. This lower conductivity level obtained for FP

materials suggests that the freeze–drying process leads to weaker electrical contacts efficiency between carbon nanotubes. This could be the result of a higher residual surfactant amount in the case of freeze–dried materials. Indeed, the organization of this surfactant in the film is highly uncertain [35–38]. One can suppose that a part is dissolved in the polymer and an other part is adsorbed on nanotubes surface. The FP process may prevent exudation of surfactant (as occurs during the slow evaporation) and may lead to a higher amount of surfactant adsorbed on nanotube surface. This adsorbed surfactant could strongly modify properties of tube–tube contacts.

When this 3 vol% of MWNTs filled FP composite is stretched, $\sigma'_e$ rapidly decreases and a very small peak of $\sigma''_e$ appears at low deformation. Then, for deformations higher than 0.5, the dielectric behavior of the matrix is found. Moreover, no increase in conductivity is observed for the first deformation levels, as for the *E* composite, which is consistent with the assumption of less entanglements between nanotubes in the FP composite. Indeed, the stretching of an entangled nanotube network will lead to the nanotube rearrangement (increase of contacts) because of the cooperative effects between entangled nanotubes. This explain the increase in conductivity observed at the first stage of deformation in the *E* material. On the other hand, when nanotubes are isolated from each other within a soft polymer matrix, the material stretching will only induce a nanotube alignment, which would tend to reduce the conductivity of the sample. This last case corresponds to the FP material where carbon nanotubes were assumed to be less entangled.

## 4. Concluding remarks

The mechanical behavior under large deformation of poly(styrene-*co*-butyl acrylate) reinforced by high aspect ratio flexible nanofibers was studied. By studying two different types of fibers with two processing routes, *E* or FP, two main effects were highlighted: the role of the interactions existing at contacts between nanofibers and the influence of fiber entanglements. Different assumptions were made and found consistent with the experimental results.

A high reinforcement effect is achieved for cellulose filled *E* materials, suggesting the presence of a rigid cellulose nanofibril network, linked by strong hydrogen bonds, within the material. The formation of such a network is possible only above the nanofibril percolation threshold (which can be very low as suggested by the high nanofibrils aspect ratio) but is detectable by tensile test for cellulose content higher than 1.5 vol%. Beyond this filler content, the strength of the contacts between nanofibrills (and thus, the rigidity of the nanofibril network) governs the composite mechanical behavior. Indeed, an important decrease of the composite ultimate strain is observed for high cellulose contents. This network is irreversibly damaged for low strain level, inducing a strong decrease in the composites mechanical properties after pre-deformation.

When such strong interactions between fillers are limited by the processing conditions (FP systems with cellulosic fillers), the resulting reinforcement effect is less important but no decrease of the ultimate strain is observed. Indeed, in that case, composite irreversible damage is not observed after a pre-deformation. The material behaves as a more classical composite filled with high aspect ratio fibers isolated from each other. The mechanical reinforcement is due to stress transfer from the matrix through the fillers.

With carbon nanotubes as fillers, the role of entanglements between nanofibers was investigated. Indeed, no strong interactions are possible between MWNTs. The FP process was assumed to prevent entanglement formation between MWNTs to explain experimental differences between *E* and FP materials. The soft entangled nanotube network (in *E* systems) was found to have an influence on the composite tensile behavior only at high temperatures. Such a soft network is efficient for mechanical reinforcement when the polymer matrix is highly viscous. At room temperature, the mechanical reinforcement can be modeled by a classical mean field approach and is equivalent whatever the processing conditions (i.e. whatever the nanotube entanglement rate).

Nevertheless, for such conductive nanofibers like carbon nanotubes, an experimental device was developed to follow the composites Ac electrical properties during the tensile tests. The electrical conductivity level of conductive fillers/insulating matrix composites is mainly influenced by the filler/filler contact properties. The efficiency of the tube/tube electrical contacts was found to be largely better in *E* materials. Moreover, the entangled structure of *E* materials brings to a wide deformation range where the material remains highly conductive. The decrease of the electrical properties is related to the disentanglement of the carbon nanotube percolating network. Conversely, for FP systems where electrical contact properties are weaker and where less entanglements are created between nanotubes, the material looses its electrical 'sensitivity' for lower deformation levels, i.e. its electrical properties rapidly decrease (down to those of the pure matrix) with the strain.

## Acknowledgements

The authors would like to thank Mr C. Graillat (LCPP-CPE Lyon) for his help and his fruitful advises in latex synthesis, as well as M. Kneveler for his contribution to some experimental data. They also acknowledge I. Paintrand and M.-F. Marais (CERMAV, Grenoble, France) for their help in cellulose processing and characterization; and *E*. Couteau and A. Magrez (IPCM, EPFL, Switzerland) for the preparation of carbon nanotubes. The work in Lausanne was supported by the Swiss National Science Foundation and its NCCR 'Nanoscale Science'. This work is performed in the frame of the European CNT-network and the GDRE no. 2756 'Science and applications of the nanotubes—NANO-*E*'.

## References

[1] Chazeau L, Gauthier C, Vigier G, Cavaillé JY. Relashionships between microstructural aspects and mechanical properties of polymer-based nanocomposites. Handbook of organic–inorganic hybrid materials and

nanocomposites, vol. 2. California, USA: American Scientific Publishers; 2003.
[2] Favier V, Canova G, Shrivastava S, Cavaillé JY. Polym Eng Sci 1997; 37(10):1732–9.
[3] Hajji P, Cavaillé JY, Favier V, Gauthier C, Vigier G. Polym Compos 1996;17(4):612–9.
[4] Itoh T, Brown RMJ. Planta 1984;160:372–81.
[5] Neville AC. Biology of fibrous composites. New York: Cambridge University Press; 1993.
[6] Vincent JFV. J Exp Biol 1999;202:3263–8.
[7] Eichhorn SJ, Young RJ. Cellulose 2001;8:197–207.
[8] Dinand E, Chanzy H, Vignon MR. Cellulose 1996;3:183–8.
[9] Dufresne A, Vignon MR. Macromolecules 1998;31(8):2693–6.
[10] Ijima S. Nature 1991;354:56–8.
[11] Yu MF, Files BS, Arepalli S, Ruoff RS. Phys Rev Lett 2000;84(24):5552–5.
[12] Salvetat JP, Bonard JM, Thomson NH, Kulik AJ, Forro L, Benoit W, et al. Appl Phys A 1999;69:255–60.
[13] Demczyk BG, Wang YM, Cumings J, Hetman M, Han W, Zettl A, et al. Mater Sci Eng A 2002;334:173–8.
[14] Zhang P, Huang Y, Geubelle PH, Klein PA, Hwang KC. Int J Solids Struct 2002;39:3893–906.
[15] Zhang P, Lammert PE, Crespi VH. Phys Rev Lett 1998;81(24):9346–9.
[16] Nardelli MB, Fattebert JL, Orlikowski D, Roland C, Zhao Q, Bernholc J. Carbon 2000;38:1703–11.
[17] Jia Z, Wang Z, Xu C, Liang J, Wei B, Wu D, et al. Mater Sci Eng A 1999; 271:395–400.
[18] Cooper CA, Ravich D, Lips D, Mayer J, Wagner HD. Compos Sci Technol 2002;62:1105–12.
[19] Pötschke P, Fornes TD, Paul DR. Polymer 2002;43:3247–55.
[20] Thostenson ET, Ren Z, Chou TW. Compos Sci Technol 2001;61:1899–912.
[21] Velasco-Santos C, Martínez-Hernández AL, Fisher F, Ruoff R, Castaño VM. J Phys D: Appl Phys 2003;36:1423–8.
[22] Kaneto K, Tsuruta M, Sakai G, Cho WY, Ando Y. Synth Met 1999;103: 2543–6.
[23] Benoit JM, Corraze B, Lefrant S, Blau WJ, Bernier P, Chauvet O. Synth Met 2001;121:1215–6.
[24] Kilbride BE, Coleman JN, Fraysse J, Fournet P, Cadek M, Drury A, et al. J Appl Phys 2002;92(7):4024–30.
[25] Sandler JKW, Kirk JE, Kinloch IA, Shaffer MSP, Windle AH. Polymer 2003;44:5893–9.
[26] Regev O, ElKati PNB, Loos J, Koning CE. Adv Mater 2004;16(3): 248–51.
[27] Dalmas F, Cavaillé JY, Gauthier C, Chazeau L, Dendievel R. Compos Sci Technol, in press.
[28] Bernholc J, Brenner D, Nardelli MB, Meunier V, Roland C. Annu Rev Mater Res 2002;32:347–75.
[29] Couteau E, Hernadi H, Seo JW, Thiên-Nga L, Miko C, Gaal R, et al. Chem Phys Lett 2003;378:9–17.
[30] Flandin L, Bréchet Y, Cavaillé JY. Compos Sci Technol 2001;61: 895–901.
[31] Halpin JC. J Compos Mater 1969;3:732–4.
[32] Eichhorn SJ, Baillie CA, Zafeiropoulos N, Mwaikambo LY, Ansell MP, Dufresne A, et al. J Mater Sci 2001;36:2107–31.
[33] Favier V, Dendievel R, Canova G, Cavaillé JY, Gilormini P. Acta Mater 1997;45(4):1557–65.
[34] Dufresne A, Cavaillé JY, Vignon MR. J Appl Polym Sci 1997;64: 1185–94.
[35] Lam S, Hellgren AC, Sjöberg M, Holmberg K, Schoonbrood HAS, Unzué MJ, et al. J Appl Polym Sci 1997;66:187–98.
[36] Steward PA, Hearn J, Wilkinson MC. Adv Colloid Interface Sci 2000;86: 195–267.
[37] Belaroui F, Hirn MP, Grohens Y, Marie P, Holl Y. J Colloid Interface Sci 2003;261:336–48.
[38] Martin LR. J Appl Polym Sci 1996;62:1893–901.